Wagley Yadav (Orcid ID: 0000-0002-1261-4267)

Canonical Notch Signaling is Required for Bone Morphogenetic Protein-mediated Human Osteoblast Differentiation

Running Title: Notch activation augments human osteoblastogenesis

Yadav Wagley[1*], Alessandra Chesi[2,3], Parker K. Acevedo[1], Sumei Lu[2], Andrew D. Wells[2,4], Matthew E. Johnson[2,3], Struan F. A. Grant[2,3,5,6,7,8], Kurt D. Hankenson[1*]

[1] Department of Orthopaedic Surgery, University of Michigan Medical School, Ann Arbor, MI 48109, [2]Center for Spatial and Functional Genomics, [3]Division of Human Genetics, and [6]Division of Diabetes and Endocrinology, The Children's Hospital of Philadelphia, Philadelphia, PA 19104; [4]Department of Pathology and Laboratory Medicine, [5]Department of Pediatrics, [7]Institute of Diabetes, Obesity and Metabolism, and [8]Department of Genetics, Perelman School of Medicine, University of Pennsylvania, Philadelphia, PA 19104

* **Corresponding authors**: Yadav Wagley, PhD, ywagley@med.umich.edu, Kurt D. Hankenson, DVM, PhD, 109 Zina Pitcher Pl, Rm 2019 Biomedical Sciences Research Building, University of Michigan Medical School, Ann Arbor, MI 48109, kdhank@umich.edu

Author Contributions:

Conception and design: Yadav Wagley, Struan F. A. Grant, Kurt D. Hankenson

Financial Support: Struan F. A. Grant, Kurt D. Hankenson

Administrative support: Andrew D. Wells, Struan F. A. Grant, Kurt D. Hankenson

Collection and/or assembly of data: Yadav Wagley, Alessandra Chesi, Parker K. Acevedo, Matthew E. Johnson, Sumei Lu

Data analysis and interpretation: Yadav Wagley, Alessandra Chesi, Parker K. Acevedo, Andrew D. Wells, Matthew E. Johnson, Struan F. A. Grant, Kurt D. Hankenson

Manuscript writing: Yadav Wagley, Alessandra Chesi, Matthew E. Johnson, Struan F. A. Grant, Kurt D. Hankenson.

Final approval of manuscript: Yadav Wagley, Alessandra Chesi, Parker K. Acevedo, Sumei Lu, Andrew D. Wells, Matthew E. Johnson, Struan F. A. Grant, Kurt D. Hankenson

Disclosures: K.D.H. declared research funding from Orthofix. All of the other authors declared no potential conflict of interest.

Acknowledgements: Some of the materials employed in this work were provided by the Texas A&M Health Science Center College of Medicine Institute for Regenerative Medicine at Scott &

White through a grant from ORIP of the NIH, Grant # P40OD011050. This work was in part funded by the Department of Defense CDMRP W81XWH-15-1-0689. S.F.A.G is funded by the Daniel B. Burke Endowed Chair for Diabetes Research.

ABSTRACT

Osteoblast differentiation of bone-marrow derived human mesenchymal stem cells (hMSC) can be induced by stimulation with either canonical Notch ligand, Jagged1, or bone morphogenetic proteins (BMP). However, it remains elusive how these two pathways lead to the same phenotypic outcome. Since Runx2 is regarded as a master regulator of osteoblastic differentiation, we targeted Runx2 with siRNA in hMSC. This abrogated both Jagged1 and BMP2 mediated osteoblastic differentiation, confirming the fundamental role for Runx2. However, while BMP stimulation increased Runx2 and downstream Osterix protein expression, Jagged1 treatment failed to upregulate either, suggesting that canonical Notch signals require basal Runx2 expression. To fully understand the transcriptomic profile of differentiating osteoblasts, RNA sequencing was performed in cells stimulated with BMP2 or Jagged1. There was common upregulation of *ALPL* and extracellular matrix genes, such as *ACAN*, *HAS3*, *MCAM*, and *OLFML2B*. Intriguingly, genes encoding components of Notch signaling (*JAG1*, *HEY2* and *HES4*) were among the top 10 genes upregulated by both stimuli. Indeed, *ALPL* expression occurred concurrently with Notch activation and inhibiting Notch activity for up to 24 hours after BMP administration with DAPT (a gamma secretase inhibitor) completely abrogated hMSC osteoblastogenesis. Concordantly, RBPJ (Recombination Signal Binding Protein for Immunoglobulin Kappa J Region, a critical downstream modulator of Notch signals) binding could be demonstrated within the *ALPL* and *SP7* promoters. As such, siRNA mediated ablation of RBPJ decreased BMP-mediated osteoblastogenesis. Finally, systemic Notch inhibition using diabenzazepine (DBZ) reduced

BMP2-induced calvarial bone healing in mice supporting the critical regulatory role of Notch signaling in BMP-induced osteoblastogenesis.

Keywords: Runx2, Notch signaling, bone morphogenetic proteins, human mesenchymal stem cells, osteoblasts

Significance Statement:

While BMPs are potent osteoblastogenic agents, the role for Notch signaling in osteoblastogenesis has been controversial. In addition to activating canonical SMAD protein, BMPs also lead to increased Notch receptor processing, Notch target gene expression, and Notch ligand Jagged1 upregulation. Blocking canonical Notch signaling ablates BMP-induced osteoblastogenesis but not BMP signaling. Given that Jagged1 stimulation alone drives osteoblastic differentiation of hMSCs, and that loss-of-function mutations in the Jagged1 gene causes low bone mass and osteopenia in humans, decreases in Jagged1 ligand during osteoblastogenesis may contribute to reduced bone formation by affecting activity of classical osteoanabolic factors, such as BMP.

INTRODUCTION

Signaling molecules that play a major role in patterning of the developing embryo are capable of significantly affecting osteoblast differentiation of primary bone marrow-derived mesenchymal progenitor cells (MSCs) [1]. These include members of the bone morphogenetic protein (BMP) family, the transforming growth factor β (TGF-β) superfamily, fibroblast growth factors (FGFs), the Wnt family of secreted factors, and hedgehog and Notch pathway ligands [2 3]. It is now well established that integration of multiple signals with sequential activation of transcription factors during various stages of differentiation is key to properly drive osteoblastogenesis [2].

Since their initial discovery over 60 years ago, over 20 BMP family members have been identified and characterized [4]. Studies in transgenic and knockout mice and in humans with naturally occurring mutations have established that BMP signaling also impacts heart, neural and cartilage development apart from their role in postnatal bone formation [4 5]. Among the BMP family members, BMP2, BMP4, BMP6, BMP7 and BMP9 are all known to promote osteoblastic differentiation of MSCs both *in vitro* and *in vivo* [6]. Upon ligand binding, BMPs recruit a hetero-tetrameric receptor complex and initiate a canonical signal transduction cascade consisting of SMAD and TAK1 dependent signaling (leading to the activation of mitogen-activated protein kinase (MAPK)) that converge on classical osteoblastic transcription factors Runx2, Dlx5 and Osterix to orchestrate osteoblast differentiation of MSCs [3 7]. In addition, BMP signals crosstalk with Wnt, Hedgehog, PTHrP, FGF and Notch signaling to co-ordinate bone homeostasis *in vivo* [7].

Notch signaling is a key cell-to-cell communication pathway that controls multiple stem-cell fates such as proliferation, self-renewal, and differentiation during embryonic development and postnatal life [8]. Ligand-mediated Notch activation involves a series of proteolytic cleavages of the Notch family of receptors (Notch 1-4) in signal receiving cells, which releases the intracellular Notch domain into the cytoplasm (NICD) [9]. The released NICD translocates from the cytoplasm to the nucleus and initiates transcription of the Notch target genes by interacting with DNA binding CSL/RBP-J protein, MAML (the transcriptional coactivator, mastermind-like-1), and other transcription factors [10]. Previous studies examining the role of Notch signaling in osteoblast differentiation often have produced conflicting reports. However, abolishing Notch ligand Jagged-1 signaling in mouse models has successfully recapitulated some of the skeletal abnormalities seen in Alagille patients, who harbor inactivating mutations of Jagged1 [11 12]. In agreement with Notch signaling being osteoanabolic, reports from our laboratory have shown that culturing hMSC in presence of Jagged1 induces osteoblast differentiation via a PKC delta dependent mechanism [10 13] and that intraoperative delivery of the Notch ligand Jagged1 using collagen scaffolds regenerates appendicular and craniofacial bone defects in rodents [14].

In recent years, increasing number of studies have reported that BMP and Notch signals crosstalk with each other to either enhance [15 16] or antagonize each other [17] during osteogenesis. Hill et al. observed that Jagged1 knockout in mouse cranial neural crest cells caused maxillary hypoplasia, and inhibiting Jagged1 expression significantly decreased the mineralization potential of mouse embryonic maxillary mesenchymal cells in response to BMP stimulation [18]. Moreover,

Hey1, a canonical Notch target gene can be induced by BMP stimulation of hMSCs, MC3T3, C2C12 and in mouse calvarial cells [19]. Since most of BMP-Notch crosstalk studies are based on rodent models, there is a paucity of data in the human setting. Although clear skeletal malformations are observed in patients with Alagille syndrome, who harbor inactivating Notch mutations, it is not clear if canonical Notch signals co-operate with canonical BMP signals and/or classical osteogenic transcription factors Runx2 and Osterix. Herein we explored the transcriptomic profile of differentiating human osteoblasts and discovered that canonical Notch signal itself is a major driver of human osteoblastogenesis and has a major regulatory role during BMP stimulation of hMSCs. Our results demonstrate that BMP signaling results in concomitant activation of Notch signaling and alkaline phosphatase expression, and that blocking Notch signaling abrogates early-phases of human osteoblast differentiation.

Materials and Methods

Culture and treatment of human mesenchymal stem cells:

Primary bone-marrow derived human mesenchymal stem cells (hMSC) derived from healthy donors (age range 22 years to 29 years) pre-characterized for cell surface expression (CD166+ CD90+ CD105+ CD36- CD34- CD10- CD11b- CD45-) and tri-lineage differentiation (osteoblastic, adipogenic and chondrogenic) potential at the Institute of Regenerative Medicine, Texas A&M University were used throughout the study. For routine maintenance of hMSCs, cells

were cultured at a density of 3000 cells/cm^2 using alpha-MEM supplemented with 16.5% FBS (Atlas Biologicals, CO) in standard culture conditions. Jagged1 (R&D Systems, MN) stimulation was carried out by immobilizing recombinant human Jagged1 onto tissue culture plates with minor modifications as previously described [10 13], whereas bone morphogenetic protein (BMP) stimulation was carried out by adding 300 ng/ml of recombinant human/mouse/rat BMP-2 or BMP-6 (R&D Systems, MN) to the cultured cells. Briefly, recombinant human Jagged1 (5 µg/ml in sterile phosphate buffered saline) solution was coated onto tissue culture plates for 1 h at 37ºC. hMSC harvested from routine maintenance media were re-suspended at a density of 60,000cells/ml using serum-containing osteogenic media (routine maintenance media additionally supplemented with 25 µg/ml Ascorbic acid-2-phosphate (AA2P), 5 mM beta-glycerophosphate (BGP) and 1% insulin-transferrin-selenous acid (ITS)) and directly plated onto the Jagged1 coated dish. After 3 days of Jagged1 stimulation, cells were harvested for RNA, protein, histochemical alkaline phosphatase detection or received fresh osteogenic media (every 2 days after the first 3 days) until stained for alizarin red S (typically within 10 days after plating the cells onto the Jagged1 coated dish). For BMP treatment, 15,000 cells/cm^2 were plated using serum-containing osteogenic media for 2 days and stimulated with recombinant BMPs (300 ng/ml) in serum-free osteogenic media. BMP stimulated cells were harvested after 3 days for RNA and protein, and after 3-4 days for histochemical alkaline phosphatase detection or received fresh serum-free osteogenic media (every 2 days after the first 3 days) until stained for Alizarin red S (typically within 10 days after BMP stimulation).

Small interfering RNA transfection of hMSCs:

Small interfering RNA for Runx2 was purchased from Ambion (Cat. No: AM16708) and set of 4 ON-TARGETplus Human RBPJ siRNA (LQ-007772-00-0002) was obtained from Dharmacon Inc. One day before siRNA transfection, 60,000 hMSCs were seeded onto each well of a 12-well plate using hMSC maintenance media and the next day transfected using DharmaFECT1 transfection reagent (Dharmacon Inc., Lafayette, CO) following manufacturer's instructions. siRNA transfected cells were allowed to recover for 2 days and either directly stimulated with 300 ng/ml of BMP (using serum-free osteogenic media) or collected by trypsinization and replated onto Jagged1 coated dishes using osteogenic media containing serum. Total RNA and protein were harvested from the transfected cells after 3 days of stimulation with Jagged1 or BMP2. Histochemical alkaline phosphatase expression was also determined at 3 days post stimulation. For Alizarin red S staining, cells received fresh osteogenic media every other day after 3 days of stimulation for 8-10 days.

Alkaline Phosphatase and Alizarin Red Staining:

At the end of treatment period (after 3-4 days depending on the experiment), multi-well plates were processed for alkaline phosphatase staining using Leukocyte Alkaline Phosphatase Kit (SIGMA) following manufacturer's instructions. For Alizarin Red S staining (usually at day 10 after treatment), each well was gently washed with PBS and fixed for 1 h using 4% neutral buffered paraformaldehyde solution. The fixative solution was removed from each well, rinsed once with

deionized water and an Alizarin Red S solution (1%, pH = 4.2) was added for 20 minutes. Excess stain solution was aspirated from each well and rinsed twice with deionized water. Stained plates were allowed to air-dry for 24 hours before processing for digital image analysis.

Relative Alkaline phosphatase stain and Alizarin red S stain was digitally quantified as described previously [20] . Each stained well was scanned using high-resolution color brightfield objective (1.25X) of the Lionheart FX automated microscope (BiotTek). For each scanned well, Image J software was used to digitally enumerate integrated density values within cell monolayers according to the guidelines provided by the National Institute of Health. Data was combined from at least 3 different donor lines and represented as average fold-change.

Quantitative RT-PCR analysis:

Total RNA was isolated from stimulated cells using TRIzol reagent (Invitrogen, CA) and quantified using a NanoDrop 2000 spectrophotometer (Thermo Scientific). 600 ng of total RNA was reverse transcribed using High Capacity cDNA Reverse Transcription Kit (Applied Biosystems) in a 20 µl reaction. The resulting cDNA was diluted three times and one microliter was amplified using Power SYBR® Green PCR Master Mix and gene-specific primers in a 7500 Fast Real-Time PCR System (Applied Biosystems) following manufacturer's recommendations. The sequences of primers used are provided in the supplementary information. Relative expression for each gene was normalized against GAPDH and expressed as fold change over control. Data from at least 3 different donor lines were combined and reported as mean±standard deviation.

Immunoblotting:

Immunoblotting was performed using standard procedures as described previously [20][21]. Briefly, hMSC monolayers were washed three times with ice-cold PBS, and lysis buffer composed of 50 mM Tris-Cl, 150 mM NaCl, 0.1% SDS, 0.1% Igepal CA 630, 0.5% sodium deoxycholate, and protease inhibitor cocktail (Roche) was added. Cell lysates were collected, vortexed vigorously, and clarified by centrifugation. The protein concentrations in the supernatant were determined using BCA protein assay (Pierce). 10-20 micrograms of each lysate were loaded into SDS-polyacrylamide gels and electro transferred onto polyvinyl difluoride membranes. Membranes were blocked for 1 h in 2.5 % non-fat skim milk in T-TBS (Tris-buffered saline containing 0.01% Tween-20), then incubated overnight at 4 ˚C with primary antibodies (see below for antibody information). Membranes were washed three times with T-TBS, then incubated with horse-radish-peroxidase conjugated secondary antibodies for 1 h at room temperature. Finally, the blots were incubated for 5 min in Supersignal™ West Femto Chemiluminescent Substrate (Fisher Scientific) and data were captured on Bio-Rad Chemi Doc system using appropriate settings for each antibody. Relative band intensities from each blot were calculated using Image Lab software v5.2.1 (Bio-Rad) and data from 3-4 different donor lines were combined for statistical analysis. The following primary and secondary antibodies were used: RUNX2 (D1L7F) Rabbit mAb (Cell Signaling Technology, 12556S, 1:1000); Anti-SP7/Osterix antibody-ChIP Grade (Abcam,

ab22552, 1:3000), RBPSUH (D10A4) XP® Rabbit mAb (Cell Signaling Technology, 5313S, 1:1000), Phospho-SMAD1 (Ser463/465)/Smad5 (Ser463/465)/Smad9 (Ser465/467) (D5B10) Rabbit mAb (Cell Signaling Technology, 13820S, 1:1000), Cleaved Notch1 (Val1744) (D3B8) Rabbit mAb (Cell Signaling Technology, 4147S, 1:1000), Notch2 (D76A6) XP® Rabbit mAb (Cell Signaling Technology, 5732S, 1:2000), Notch3 (D11B8) Rabbit mAb (Cell Signaling Technology, 5276S, 1:3000), GAPDH (Cell Signaling Technology, 5174S, 1:30000), Anti-rabbit IgG, HRP-linked antibody (Cell Signaling Technology, 7074S, 1:5000), and Anti-mouse IgG, HRP-linked antibody (Cell Signaling Technology, 7076S, 1:5000).

RNA sequencing:

Total RNA was isolated from cells stimulated with Jagged1 or BMP for 3 days using TRIzol reagent following manufacturer's instructions. RNA clean-up and on-column DNase digestion was performed using RNeasy® Mini-Kit (Qiagen) following standard procedures. Total RNA samples were processed for library preparation and sequencing as previously described [20]. Briefly, rRNA was depleted from the total RNA samples using Ribo-Zero rRNA Removal Kit (Illumina). RNA-seq libraries were prepared using the NEBNext Ultra II Directional RNA library Prep Kit for Illumina (NEB) following standard protocols. Libraries were sequenced on one S2 flow cell on an Illumina NovaSeq 6000, generating ~200 million paired-end 50 bp reads per sample. RNA-seq data were aligned to the hg19 genome with STAR v.2.5b [22] and pre-processed with PORT (https://github.com/itmat/Normalization) using the GENCODE Release 19 (GRCh37.p13)

annotation plus annotation for lincRNAs and sno/miRNAs from the UCSC Table Browser (downloaded 7/7/2016). Normalized PORT counts for the uniquely mapped read pairs to the sense strand were additionally normalized by gene size and the resulting values were used in the computation of gene expression percentiles.

Chromatin Immunoprecipitation:

Chromatin Immunoprecipitation (ChIP) assays were performed as reported previously with minor modifications [23] . Briefly, 2 X 10^6 hMSCs stimulated with or without BMP2 for 72 h were collected by trypsinization and chromatin complexes were crosslinked by the addition of 1% formaldehyde for 15 minutes. Formaldehyde fixing was quenched by addition of cold glycine (final concentration - 125 mM), and the cells were collected by centrifugation. Cells were lysed (25 mM HEPES, 1.5 mM $MgCl_2$, 10 mM KCl, 0.1% NP-40, 1 mM DTT, 0.5 mM PMSF, and protease inhibitors) on ice for 10 minutes to isolate nuclei. Nuclei were re-suspended in sonication buffer (50 mM HEPES, 140 mM NaCl, 1 mM EDTA, 1% Triton X-100, 0.1% sodium deoxycholate, 0.1% SDS, and protease inhibitors) and sonicated 20-cycles (30 second pulse, 30 second rest on a Bioruptor pico, Diagenode) to isolate chromatin. Clarified chromatin was divided into two fractions after saving 10% as input samples, and 1 µg of Normal Rabbit IgG (Cell signaling Technology, 2729S) or RBPJ antibody (Cell signaling Technology, 5313S, 1:50 dilution) were added. The chromatin antibody complexes were incubated overnight at 4ºC on a rotating platform. Next day, protein G dynabeads (pre-blocked with 5% BSA, 30 µl per

immunoprecipitation condition) were added to capture the immune complexes for 1 h at 4ºC. The magnetic beads were extensively washed in a series of low- and high-salt wash buffers, LiCl wash buffer and Tris-EDTA buffer. The immune complexes were eluted, decrosslinked (overnight at 65ºC), and treated with RNase for 30 minutes. Finally, DNA was purified from the eluate by using a Qiagen PCR cleanup kit (Cat. No. 28106). Each immunoprecipitated DNA sample was analyzed by real-time qPCR using specific primers (sequences are provided in the supplementary information and spanned regions containing putative RBPJ consensus sequence except for *RUNX2* promoter, where it couldn't be identified). ChIP assays were repeated in three unique hMSC donor lines and relative enrichment for each condition was calculated using standard procedure.

Calvarial defect model:

All animals in this study were used in compliance with the University of Michigan guidelines and approved IACUC protocol. A group of C57Bl6 mice (n=18, age 14-20 weeks) underwent calvarial defect surgery as briefly described below. At the time of surgery, animals were anesthetized and a 3 mm defect was drilled into each parietal bone using a piezo drill. A collagen sponge graft (Advanced Biomatrix SpongeCol 5135) was loaded with a solution containing 0.25 μg BMP2 and placed over the bone defect, and the incision was closed. Post-surgical, animals were closely monitored and received Buprenorphine injections every 12 hours for the next 48 hours. After 5 days of surgery, animals were randomly assigned into groups and treated daily for the next 5 days with either 10 μg/kg Diabenzazepine (DBZ) or a vehicle control via intraperitoneal injection as

described previously for *in vivo* Notch inhibition [24]. After 42 days, whole calvariae were removed and fixed in 4% paraformaldehyde for 48 hours. Fixed calvariae were briefly rinsed with distilled water and transferred to 70% ethanol until scanned. Scanned microCT images were analyzed using Parallax Microview software and the extent of new bone formation determined as described previously [14].

Statistical analysis:

Numerical values for each assay are reported as mean ± standard deviation. The number of donors assessed and replicates used for each experimental condition are mentioned in figure legends. A 2-way homoscedastic Student's *t*-test was performed to determine significant differences among experimental conditions. * represents significant difference ($P \leq 0.05$) compared to control, and # represents significant difference between experimental groups ($P \leq 0.05$).

RESULTS

Runx2 abrogation inhibits both Jagged1 and BMP mediated human osteoblast differentiation:

We have previously demonstrated that Jagged1 induces hMSC osteoblast differentiation through canonical Notch signaling and requires concomitant PKCdelta signaling [10] [13]. However, the role of osteoblast specific transcription factor Runx2 during Jagged1 induced hMSC osteoblast differentiation is unknown. We introduced siRNA against Runx2 in hMSC and stimulated targeted

cells with Jagged1 or BMP2 for 3 days after which ALP staining was carried out. Parallel plates received fresh osteogenic media until assessed for mineralization within 8-10 days. The 3 day time-point was chosen for histochemical ALP detection because earlier studies from our laboratory have demonstrated that the maximal ALP expression in BMP or Jagged1 stimulated hMSCs occurred between 72-96 hours after stimulation [10 25-27]. As shown by histochemical staining in figures 1A-1D (and respective quantification in the histograms below the scanned images), Runx2 silencing efficiently reduced both Jagged1 and BMP2 mediated ALP expression and extracellular matrix mineralization. Corresponding to staining results, quantitative RT-PCR analysis also revealed significant reduction of *ALPL* gene expression levels in Runx2 silenced cells (Supplementary figure 1A and 1D). Despite the reduction in alkaline phosphatase expression and reduction of extracellular calcium deposition in Runx2 silenced cells, the expression levels of canonical targets *HES1, HEY1* (canonical Notch target genes) and *ID1* (canonical BMP target gene) were not affected (instead the levels of *HES1* and *ID1* were further enhanced) (supplementary figure 1B, 1C and 1E) suggesting Runx2 directly regulates the osteoblastogenic fate of hMSCs in both Jagged1 and BMP treated cells, but does not directly affect signaling.

To examine how Runx2 and Osterix (a downstream transcription factor for osteoblast differentiation) proteins are modulated under Notch stimulation, we prepared total cell lysate from non-targeted cells or Runx2 targeted cells and performed immunoblotting. Runx2 and Osterix were expressed in untreated cells and the levels of Runx2 and Osterix protein in control siRNA transfected cells significantly increased upon BMP2 stimulation (Figure 1E-G), but their levels

stayed relatively constant during Jagged1 stimulation (Figures 1H-J). As expected, Runx2 protein levels were very low in Runx2 siRNA targeted cells, both in basal and under stimulated conditions. Additionally, although Runx2 siRNA reduced Osterix expression mediated by BMP2 stimulation to baseline levels, the basal Osterix expression levels remained unchanged with Runx2 siRNA in both BMP2 and Jagged1 treated cells (Figures 1E, 1G, 1H, 1J, lanes 1 and 3). To demonstrate Notch processing was unaltered by Jagged-1 stimulation of Runx2 silenced cells, the levels of active Notch1 protein (Notch1 val1744) and Notch2 NTM (the transmembrane fragment generated before gamma secretase cleavage) were also determined (Figure 1H). Taken together, this suggest that although Runx2 is not required for basal Osterix expression, canonical Notch and BMP signals interact with endogenous Runx2 protein to initiate human osteoblast differentiation.

Jagged1 and BMP2 stimulations result in the differential expression of relatively few common genes (RNA-seq)

Considering that both Notch signaling and BMP signaling can mediate terminal osteoblastogenesis and were blocked by Runx2, we conducted RNA-seq on three unique donor lines after 3 days of stimulation with Jagged1 and BMP2 to understand the transcriptomic profile of differentiating osteoblast. We chose 3 days of stimulation with each ligand because the expression of *ALPL* is highly elevated at this time-point but the cells have not yet mineralized. As summarized in figure 2A, BMP2 treatment resulted in differential expression of 2906 genes (fold change 1.5 at a false discovery rate of <10%) of which 1749 were upregulated and 1157 were down regulated (Figure 2A and Supplementary Table 1). Compared to BMP2, relatively fewer genes showed differential

regulation- 342 genes were differentially expressed, and included 167 upregulated, and 175 down regulated (Figure 2A and Supplementary Table 2). Rather surprisingly, the genes that were co-expressed by both stimulations were relatively limited, and only 45 genes showed common upregulation and 69 showed common downregulation (Figure 2B, supplementary figure 3, 6 and supplementary table 3). *ALPL* was among the top 10 commonly upregulated genes and also included a set of early osteoblast-associated genes including *ACAN*, *HAS3*, *MCAM* and *OLFML2B* (Figures 2C and 2D). It was particularly intriguing that three Notch signaling genes (*JAG1*, *HEY2* and *HES4*) were among the top 10 commonly upregulated genes (Figure 2C and 2D) and also included *NOTCH3* within the top 45 suggesting Notch activation by both BMP2 and Jagged1 during human osteoblast differentiation (supplementary tables 1, 2 and 3). Finally, two of the top 10 commonly upregulated genes were a transcriptional regulator *ID4* and *NPTXR*, a gene known to be involved in synaptic modulation (Figure 2C and 2D). Strikingly, Ingenuity Pathway Analysis of the top 45 commonly upregulated genes showed a similar trend obtained with the top 10 commonly upregulated genes. The top 3 highly upregulated pathways were Notch signaling, Regulation of the Epithelial-Mesenchymal Transition Pathway, and Osteoarthritis pathway (Figure 2C, Supplementary Figures 2 and 3). Furthermore, consistent with immunoblot results for Runx2 and Osterix (Figure 1H), it was notable that while BMP2 upregulated *RUNX2*, *SP7* (Osterix), *SPP1*, *SOST*, *DKK1* and *DMP1* (classical genes implicated in differentiated osteoblasts), expression levels of these genes did not significantly change in Jagged1 stimulated cells (supplementary tables 1and 2 and data not shown).

Next, we also considered the possibility of osteoblastic differentiation regulation by commonly downregulated genes. Among the top 10 commonly downregulated genes, we observed that 3 of the genes were SH3 domain containing proteins (*SH3D19*, *UBASH3B*, and *SH3BP5*) (supplementary table 3), which are known to affect protein phosphorylation. Intriguingly, *SH3D19* is also known to be involved in regulating ADAMs (A disintegrin and metalloprotease) [28] which affects the Notch signaling pathway. Considering upregulation of Notch signaling components in response to both BMP2 and Jagged1, we chose to further study the role of Notch in BMP mediated hMSC osteoblastogenesis.

Notch signaling is required for BMP-mediated osteoblastogenesis

Considering the upregulation of Notch signaling related genes by BMP revealed by RNA-seq, we determined if Notch signaling was required for BMP2-mediated human osteoblast differentiation. Cells were treated with DAPT (a gamma secretase inhibitor that blocks the generation of Notch intracellular domains) simultaneously with BMP (BMP2 and BMP6) at various time points after BMP stimulation. At the end of 96 h, alkaline phosphatase expression was histochemically determined. As shown in figure 3A, alkaline phosphatase expression in response to BMP was inhibited even when DAPT was added as late as 24 hours after BMP stimulation (Figure 3A). However, this inhibitory effect was gradually lost from 24 to 48 hours and no apparent reduction on alkaline phosphatase expression could be observed when DAPT was added 72h after BMP stimulation (Figure 3A). In a parallel set of experiment, extracellular matrix mineralization was determined by Alizarin red staining after 10 days (Figure 3B). As observed above for alkaline

phosphatase expression, simultaneous DAPT treatment completely blocked BMP-mediated extracellular calcium deposition (Figure 3B) and such inhibitory effect was maintained even when DAPT was added 24 h after the initial BMP treatment (Figure 3B). Notably, gamma-secretase inhibition became ineffective after 48 h of BMP stimulation and both alkaline phosphatase and extracellular calcium deposition are unchanged in cells treated with DAPT after 48 h of BMP stimulation. In corresponding experiments, we determined how gamma secretase inhibition affected the expression of canonical BMP target gene *ID1* (as well as *ALPL*) and examined how it affected the Notch target genes identified from our RNA-seq data, *HEY2* and *HES4*. As shown in figures 3C, 3D, 3E and 3F, despite minimal effects on the BMP-mediated expression levels of *ID1* (Figure 3C) by DAPT, the expressions of *ALPL*, *HEY2* and *HES4* were significantly reduced by blocking Notch signaling with DAPT in the presence of BMP2. Further quantitative gene expression analysis on the top 10 commonly upregulated genes by BMP2 and Jagged1 also showed reductions in BMP2 and DAPT co-stimulated cells (data not shown).

To investigate whether Notch proteins are activated by BMP stimulation and to assess the combined effect of gamma secretase inhibition on BMP signal transduction, we conducted immunoblotting experiments from cell lysate prepared after co-stimulation with BMP2 and DAPT. At first, we examined the effect of DAPT on BMP-mediated SMAD protein phosphorylation. As shown in figure 3G and 3H and supplementary figures 4A and 4B (first panel), there was no significant difference on the levels of SMAD phosphorylation elicited by BMP proteins in the presence of DAPT both in short-term (1 h) or longer treatment (72 h) durations. In further

experiments, the effect of DAPT on the expression of Runx2 and Osterix protein levels were examined. As shown by immunoblot experiment and quantitative analyses in Figures 3G, 3I and 3J, DAPT did not affect the expression levels of Runx2 and Osterix but instead showed a slight increase that did not reach statistical significance. Similar to the results observed with BMP2, the effect of DAPT on BMP6 mediated Runx2 and Osterix proteins were minimal (supplementary figure 4B). Next, we also determined if Notch proteins are activated by BMP signaling by immunoblotting for Notch1, Notch2 and Notch3 proteins. Cleaved Notch1 antibody detects endogenous levels of the Notch1 intracellular domain only when released by cleavage between Gly1753 and Val1754 and is indicative of Notch1 activation. The Notch2 antibody detects transmembrane region (but not the intracellular domain generated by gamma secretase cleavage) and therefore, will show decreased expression when activated. Notch3 antibody, however, will show increased expression after gamma secretase activation as it can recognize both the transmembrane region and intracellular domain. Levels of Notch2 protein showed some reduction in BMP-stimulated samples and cleaved Notch1 and Notch3 (both full length and transmembrane) protein levels were increased by BMP stimulation (Figure 3G, lanes 1 and 2). Correspondingly, including DAPT during BMP stimulation reversed the BMP2's effect on Notch proteins (Figure 3G and 3K) suggestive of gamma secretase mediated Notch activation. Similar results were also obtained with BMP6 and showed that although Runx2 and Osterix protein expression are minimally affected, processing of Notch proteins in the presence of BMP was inhibited by DAPT (supplementary figure 4B). Collectively, these results suggest that Notch receptor cleavage is an

essential regulatory step in BMP-mediated osteoblastogenesis prior to 48 h of continuous BMP exposure.

BMP increases Notch signaling concomitant with increases in osterix and ALP

Given that BMP mediated alkaline phosphatase expression depends on Notch activation, we were interested to determine whether these two events are concurrent during osteoblast differentiation. Therefore, we devised a BMP-washout experiment to understand the minimal treatment duration of BMP required for alkaline phosphatase expression (Figure 4A). First, cells were stimulated with BMP-2 and then 4 h, 8 h, 24h, 48 h or 72 h later, received two consecutive media exchange to wash out residual BMP. At the end of 96 h, cells were stained for alkaline phosphatase expression. As shown in figure 4B and quantification in the right histogram, the minimum duration of BMP stimulation required for significant ALP expression was 24 hours, and by 48 hours the alkaline phosphatase expression levels was indistinguishable between cells that continuously received BMP for 96 hours suggesting that a 48 h of BMP treatment is required for high alkaline phosphatase expression. In corresponding experiments, we treated cells with BMP2 for various lengths of time ranging from 8h-96h and determined gene expression levels of *ALPL* and *ID1* (a canonical BMP target). Quite strikingly, *ID1* expression peaked earlier during the course of treatment (8 h) and gradually returned to baseline levels over the next 96 hours (Figure 3C), but *ALPL* expression followed a completely different course and showed gradual increase only after 48 hours of BMP stimulation (Figure 3D).

In the next set of experiments, we determined the kinetics of Notch protein activation in cells stimulated with BMP for a total of 96 h. As shown in figure 4E, although SMAD phosphorylation occurred much faster and already peaked after 1 h of BMP stimulation (Figure 3E, first panel and data not shown), Osterix protein expression started to increase only after 48 hours after BMP treatment. Strikingly, processing of Notch proteins was obvious 24 hours after BMP stimulation and was clearly evident after 48 hours when we could observe an increase of activated Notch1 and Notch 3 protein levels and corresponding decrease of Notch2 NTM protein levels. Additional RT-qPCR experiments to determine expression levels of *HEY2*, and *HES4* also showed comparable trend with Notch processing and became significant at 24 h, a similar timeline with Notch processing (supplementary figure 5A, 5B and 5C).

Given that *ALPL* expression was abrogated by gamma secretase inhibition (Figures 3A and 3D) and that alkaline phosphatase expression levels (Figures 4A and 4D) paralleled Notch activation, we postulated that Notch signaling is a critical event during BMP mediated alkaline phosphatase expression and extracellular calcium deposition. To demonstrate that the expression of Notch ligands also occurred and corresponds to the Notch processing, total RNA samples prepared from BMP stimulated cells for 8h were subjected to quantitative gene expression analysis. As shown in supplementary figure 4C, expression of *JAG1*, the most upregulated ligand of the Notch signaling pathway by osteogenic cells during bone fracture repair [10], was significantly increased by both BMP2 and BMP6. The expression of another Notch ligand *JAG2* could also be observed in BMP stimulated cells (supplementary figure 4D). Expression of Notch delta ligands (*DLL1*, and *DLL4*)

showed minimal changes in response to either BMP stimulation (supplementary figures 4E, 4F and 4G). Since both BMP2 and BMP6 increased *JAG1* expression in hMSCs, BMP stimulation of hMSCs seems to converge on Jagged1 expression followed by Notch processing and commitment to osteoblast differentiation.

Canonical Notch signals via RBPJ is required for BMP-mediated human osteoblast differentiation

To determine whether canonical Notch transcriptional signaling is required for BMP mediated osteoblastogenesis, we delivered RBPJ siRNA and examined the effect on terminal osteoblast differentiation. As shown in figures 5A and 5B (quantification data in figures 5C and 5D), blocking RBPJ significantly attenuated BMP mediated increase in alkaline phosphatase expression and extracellular calcium deposition. In further experiments, we also examined whether RBPJ silencing affected canonical BMP-SMAD signaling. As shown in figure 5E (first and second panels), while RBPJ siRNA completely reduced its corresponding protein expression, BMP mediated increase in SMAD1/5/9 phosphorylation was minimally affected suggesting that RBPJ silencing is not associated with impaired BMP-SMAD signaling. Quite intriguingly though, BMP2 stimulation did not increase Runx2 and Osterix protein levels in in RBPJ silenced cells. This effect of RBPJ knockout on BMP-mediated Runx2 and Osterix protein expression is in contrast to the result obtained with gamma secretase inhibition because BMP-mediated Runx2 and Osterix protein expression levels are not affected by DAPT and BMP co-stimulation (Figures 3G, 3I, 3J and supplementary figure 2B). Nevertheless, as shown by quantitative gene expression analysis,

the expression levels of *ID1* and *JAG1* were not affected in cells lacking RBPJ (Figure 5I and 5K) possibly because these genes are already activated by 8h after BMP stimulation (Figure 4D and supplementary 2C), but the expression levels of *ALPL* (Figure 5J) and *HEY2* (Figure 5L) (both of which showed increased expression after Notch activation (Figures 4E and supplementary 5A)) were significantly reduced. Taken together, these results suggest that RBPJ acts as a downstream regulatory molecule during BMP-mediated human osteoblast differentiation.

RBPJ is bound at the human *ALPL* and *SP7*(Osterix) promoters

Since abolishing RBPJ affected the expression of ALP, RUNX2 and Osterix protein expression in response to BMP2 stimulation, we were interested to determine whether RBPJ binds to the corresponding gene promoters. Thus, chromatin immunoprecipitation (ChIP) was carried out using hMSC cells stimulated with or without BMP2 for 72h and relative enrichment in RBPJ binding within various gene promoters of interest were determined. At first, RBPJ enrichment at the promoter of two canonical Notch target genes *HES1* and *HEY1* were examined. As shown in Figure 6A and 6B, *HES1* and *HEY1* promoter DNA region were significantly enriched with RBPJ antibody, both under basal and BMP2 stimulated conditions. In corresponding experiments, RBPJ binding at the *ALPL*, *SP7* (Osterix), and *RUNX2* gene promoters were evaluated. As shown in Figures 6C and 6D, RBPJ binding could be endogenously observed in *ALPL, SP7 (*Osterix) promoters, that did not significantly change with BMP2 stimulation. However, relative RBPJ binding in the *RUNX2* promoter region could not be observed (Figure 6E). A different promoter region further upstream in the *RUNX2* promoter region also showed no significant enrichment

above normal rabbit IgG (data not shown). Collectively, these data suggest that RBPJ binding is present in the *ALPL* and *SP7*(Osterix) promoters and thereby can directly regulate their expression in BMP2 stimulated cells.

Inhibition of Notch signaling reduces bone formation during BMP2 mediated calvarial defect healing of mice.

Finally, we were interested to determine whether Notch signaling is an important determinant of bone formation during BMP2 mediated bone defect healing in mice. Therefore, calvarial defect were created in a cohort of 18 mice and implanted with collagen sponges containing BMP2. At day 5 of the surgery, mice were randomly grouped and either received vehicle injection or diabenzazepine (DBZ, a gamma secretase inhibitor) injection for the next 5 days to block *in vivo* Notch activation [24]. This temporal injection regimen was chosen because Notch ligands and receptors are found to be increased upto day 10 after the surgery from our earlier report [29]. At day 42 of the initial surgery, calvariae was harvested and analyzed by microCT. As shown in Figure 7A, the amount of bone formation in DBZ injected mice were reduced. Quantification of the bone volume (Figure 7B) showed that new bone formed was significantly decreased by DBZ injection of BMP2 treated mice. Collectively, these data suggest that Notch signaling is also an important driver of BMP2-induced bone formation *in vivo.*

DISCUSSION

While BMP is considered a master-regulator of osteoblast differentiation, how BMP intersects with other signaling factors to regulate human osteoblast differentiation is still an active area of investigation. Our own work has shown that canonical Notch signaling in hMSC can increase osteoblastogenesis, but the interplay between Notch signaling and BMP has remained largely unexplored. In this body of work, we demonstrate that Runx2 remains a key driver of osteoblast differentiation, regardless of the osteogenic stimulus. Runx2 knockdown blocked both Jagged1 and BMP2 mediated osteoblastogenesis. Although, the role of Runx2 in BMP mediated osteoblastogeneis is well-understood [30], the requirement for Runx2 in Notch mediated osteoblastogenesis is a novel finding. Since RBPJ was also required for proper differentiation of hMSCs in response to BMP stimulation, it is quite possible that Runx2 and RBPJ intersect. Indeed, the essential role of RBPJ in osteoblastogenesis has been demonstrated by Prx-CRE mediated deletion of RBPJ in mouse osteoprogenitor cells, which led to the non-union of long bone fractures [31], similar to mice with Prx mediated deletion of BMP2 [32]. Intriguingly, during murine fracture healing [29] or in marrow ablation models [14], the expression of canonical Notch ligands increases well before mineralization. As such, it is probable that for proper osteoblastogenesis and bone formation to proceed, activated Notch, Runx2 and RBPJ proteins are required. Corresponding to this notion, removal of each of these three components in differentiating hMSCs led to inhibition of alkaline phosphatase expression and extracellular calcium deposition (Figures 1A-1D, 3A-3B, 5A-5B and data not shown). Furthermore, in BMP stimulated hMSCs these three factors are

gradually attained over 48 h because the expression of *JAG1* (supplementary figure 2C) is followed by the processing of Notch proteins after BMP stimulation and occurs concurrent with the increased expression of *ALPL* (Figures 4D and 4E). Indeed, our DAPT chase experiment supports this observation since gamma secretase inhibition by DAPT abolished alkaline phosphatase expression up to 24 h after BMP stimulation, but failed to do so after 48 h when Notch processing is complete. Correspondingly, Jagged1 stimulated hMSCs show significant *ALPL* gene expression within 24 hours after stimulation [10]. And on top of that, putative RBPJ consensus sequence (CCTGGGAA) can be found in the human *ALPL* promoter around 326-319 bp upstream of the transcription start site and our chromatin immunoprecipitation data showed that this region is indeed bound by RBPJ protein in hMSCs (Figure 6C).

Contrary to the positive effect of Notch signaling on human osteoblastogenesis, Notch signaling in mice is activated by hypoxia and has been shown to inhibit mouse MSC osteogenesis by antagonizing pro-osteogenic transcription by Runx2 [33][34][35]. This discrepancy on the effect of Notch on human and mouse MSC osteoblastogenesis is poorly understood and likely reflects differences in human and rodent cell models, or may reflect the plasticity between the four mammalian Notch receptors and the five different ligands. Further, this role of the Notch pathway might be cell stage specific because stimulation of the primary bone-marrow derived mouse MSCs with BMP-2 does not significantly increase the expression of *Jag1* and Notch target gene *Hey2* (data not shown). However, direct Jagged1 delivery using osteoconductive scaffold increases bone formation in rodent calvarial defect models and additionally as shown in this study (Figure 7)

blockage of Notch signals during BMP2 mediated calvarial defect regeneration reduces bone volume [14]. This discrepancy between in vitro studies with mouse cells and human cells supports the necessity for translating rodent studies to human model systems.

Our recent interactome study of differentiating human osteoblasts utilizing massively parallel ATAC-seq and Capture-C also supports requirement of crosstalk of BMP/SMAD signaling with other signaling pathways for proper human osteoblast differentiation [20]. As reported in the study, attenuating the expressions of *ING3* and *EPDR1*, critical pro-osteoblastic genes, had no effect on canonical BMP/SMAD signals and expression of Runx2 protein, yet terminal osteoblast differentiation was abolished. Considering the results presented herein, it is quite reasonable that BMP-Notch cross-talk is an important driver of human osteoblast differentiation because abolishing Notch activation up to 24 hours after BMP stimulation had a negative effect on terminal osteoblast differentiation. Thus, it would be interesting to determine if components of the Notch pathways are adversely affected by the lack of these novel pro-osteoblastic genes.

With regards to Jagged1 stimulation, although terminal osteoblast differentiation could be detected, increase in Runx2 and Osterix protein expression could not be observed. Since SMAD activation in response to BMP stimulation results in Runx2 and downstream Osterix expression [36], we assume that absence of SMAD/TAK1 activation with Jagged1 stimulation is the likely explanation for why Jagged1 stimulation does not impact Runx2 and Osterix expression. However, even though BMP-mediated SMAD activation was maintained, upregulation of both Runx2 and Osterix proteins were absent in RBPJ silenced cells (Figures 5E, 5G and 5H). Thus, it appears that

basal RBPJ expression may serve a non-canonical role in modulating RUNX2 and Osterix protein expression (and/or function). In partial agreement, RBPJ binding could be clearly observed at the Osterix promoter of hMSCs (Figure 6D), however we failed to detect such at the *RUNX2* promoter (Figure 6E). Further, relatively few (Figure 2B) commonly upregulated (total 45 genes) and down regulated genes (total 69 genes) were observed by RNA-seq during Jagged1-mediated osteoblastogenesis and BMP2-mediated osteoblastogenesis. However, of these genes commonly upregulated, Ingenuity Pathway Analysis revealed that they represent genes of Connective Tissue Development and Function, Organ Morphology, Organismal Development, and Skeletal and Muscular System Development and Function, as four of five top Physiological System Development and Function Pathways. As mentioned earlier, the transcriptome analysis was performed with cells that haven't begun to mineralize, thus the list of co-regulated genes may only represent key early mediators in osteoblast differentiation. Therefore, it would be interesting to perform a longitudinal experiment that focusses on teasing out differentially expressed genes at various stages of differentiation. Also, except for the *JAG1* and *ALPL*, none of the top 10 commonly upregulated gene show enriched Runx2 binding in ChIP-seq performed with immortalized hMSCs [37]. The essential role of these genes in the process of osteoblastogenesis will need to be elucidated, although one, *ALPL* is a well-recognized key mediator of osteoblast mineralization, for which we provide Notch pathway involvement using pharmacological as well as genetic evidence. Despite such, the alterations in *ACAN*, *HAS3*, *MCAM*, and *OLFMl2B* (as well as *ALPL*) also should carry profound effects on mineralization.

In the pathway analysis, whether using the top 10 commonly upregulated genes or all of the 45 upregulated genes, Notch signaling stood as the top Canonical Pathway identified as common between BMP and Notch induced osteoblastogenesis, suggesting a key role for Notch signaling in BMP-induced osteoblastogenesis. Indeed, we show that BMP induces Notch signaling, both at the gene expression and protein level, including upregulating both ligand and receptor expression, and that inhibiting Notch signaling - either at the level of receptor cleavage using DAPT or genetically by disrupting RBPJ - blocks terminal osteoblast differentiation, although it cannot be ruled out that RBPJ has non-canonical effects, as its absence does also result in a decrease in Runx2 and Osterix protein expression after BMP stimulation of hMSCs.

This work has important implications for understanding the process of osteoblastogenesis, and the interplay between Notch and BMP signaling. While BMP is a potent osteoblastogenic agent, the role for Notch signaling in osteoblastogenesis is more controversial. Humans with loss-of-function mutations in *JAG1* have decreases in bone mass and osteopenia, and it could be that the decrease in Jagged1 ligand during the process of osteoblastogenesis contributes to reduced bone formation. Indeed, mouse studies with disruption of *Jag1* in osteoprogenitor cells suggest decreases in bone volume [38]. Future studies will attempt to uncouple Notch and BMP signaling pathways in osteoblastogenesis, and to explore these intersections in animal models.

Acknowledgements

Some of the materials employed in this work were provided by the Texas A&M Health Science Center College of Medicine Institute for Regenerative Medicine at Scott & White through a grant from ORIP of the NIH, Grant # P40OD011050. This work was in part funded by the Department of Defense CDMRP W81XWH-15-1-0689. S.F.A.G is funded by the Daniel B. Burke Endowed Chair for Diabetes Research.

Data Availability Statement

The data that support the findings of this study are available on request from the corresponding author.

References:

1. Ullah I, Subbarao RB, Rho GJ. Human mesenchymal stem cells - current trends and future prospective. Biosci Rep 2015;**35**(2) doi: 10.1042/BSR20150025[published Online First: Epub Date]|.

2. Nakashima K, de Crombrugghe B. Transcriptional mechanisms in osteoblast differentiation and bone formation. Trends Genet 2003;**19**(8):458-66 doi: 10.1016/S0168-9525(03)00176-8[published Online First: Epub Date]|.

3. Chen G, Deng C, Li YP. TGF-beta and BMP signaling in osteoblast differentiation and bone formation. Int J Biol Sci 2012;**8**(2):272-88 doi: 10.7150/ijbs.2929[published Online First: Epub Date]|.

4. Wang RN, Green J, Wang Z, et al. Bone Morphogenetic Protein (BMP) signaling in development and human diseases. Genes Dis 2014;**1**(1):87-105 doi: 10.1016/j.gendis.2014.07.005[published Online First: Epub Date]|.

5. Chen D, Zhao M, Mundy GR. Bone morphogenetic proteins. Growth Factors 2004;**22**(4):233-41 doi: 10.1080/08977190412331279890[published Online First: Epub Date]|.

6. Beederman M, Lamplot JD, Nan G, et al. BMP signaling in mesenchymal stem cell differentiation and bone formation. J Biomed Sci Eng 2013;**6**(8A):32-52 doi: 10.4236/jbise.2013.68A1004[published Online First: Epub Date]|.

7. Wu M, Chen G, Li YP. TGF-beta and BMP signaling in osteoblast, skeletal development, and bone formation, homeostasis and disease. Bone Res 2016;**4**:16009 doi: 10.1038/boneres.2016.9[published Online First: Epub Date]|.

8. Androutsellis-Theotokis A, Leker RR, Soldner F, et al. Notch signalling regulates stem cell numbers in vitro and in vivo. Nature 2006;**442**(7104):823-6 doi: 10.1038/nature04940[published Online First: Epub Date]|.

9. Bray SJ. Notch signalling in context. Nat Rev Mol Cell Biol 2016;**17**(11):722-35 doi: 10.1038/nrm.2016.94[published Online First: Epub Date]|.

10. Zhu F, Sweetwyne MT, Hankenson KD. PKCdelta is required for Jagged-1 induction of human mesenchymal stem cell osteogenic differentiation. Stem Cells 2013;**31**(6):1181-92 doi: 10.1002/stem.1353[published Online First: Epub Date]|.

11. Humphreys R, Zheng W, Prince LS, et al. Cranial neural crest ablation of Jagged1 recapitulates the craniofacial phenotype of Alagille syndrome patients. Hum Mol Genet 2012;**21**(6):1374-83 doi: 10.1093/hmg/ddr575[published Online First: Epub Date]|.

12. McCright B, Lozier J, Gridley T. A mouse model of Alagille syndrome: Notch2 as a genetic modifier of Jag1 haploinsufficiency. Development 2002;**129**(4):1075-82

13. Dishowitz MI, Zhu F, Sundararaghavan HG, Ifkovits JL, Burdick JA, Hankenson KD. Jagged1 immobilization to an osteoconductive polymer activates the Notch signaling pathway and induces osteogenesis. J Biomed Mater Res A 2014;**102**(5):1558-67 doi: 10.1002/jbm.a.34825[published Online First: Epub Date]|.

14. Youngstrom DW, Senos R, Zondervan RL, et al. Intraoperative delivery of the Notch ligand Jagged-1 regenerates appendicular and craniofacial bone defects. NPJ Regen Med 2017;**2**:32 doi: 10.1038/s41536-017-0037-9[published Online First: Epub Date]|.

15. Cao J, Wei Y, Lian J, et al. Notch signaling pathway promotes osteogenic differentiation of mesenchymal stem cells by enhancing BMP9/Smad signaling. Int J Mol Med 2017;**40**(2):378-88 doi: 10.3892/ijmm.2017.3037[published Online First: Epub Date]|.

16. Liao J, Wei Q, Zou Y, et al. Notch Signaling Augments BMP9-Induced Bone Formation by Promoting the Osteogenesis-Angiogenesis Coupling Process in Mesenchymal Stem Cells (MSCs). Cell Physiol Biochem 2017;**41**(5):1905-23 doi: 10.1159/000471945[published Online First: Epub Date]|.

17. Wang N, Liu W, Tan T, et al. Notch signaling negatively regulates BMP9-induced osteogenic differentiation of mesenchymal progenitor cells by inhibiting JunB expression. Oncotarget 2017;**8**(65):109661-74 doi: 10.18632/oncotarget.22763[published Online First: Epub Date]|.

18. Hill CR, Yuasa M, Schoenecker J, Goudy SL. Jagged1 is essential for osteoblast development during maxillary ossification. Bone 2014;**62**:10-21 doi: 10.1016/j.bone.2014.01.019[published Online First: Epub Date]|.

19. Zamurovic N, Cappellen D, Rohner D, Susa M. Coordinated activation of notch, Wnt, and transforming growth factor-beta signaling pathways in bone morphogenic protein 2-induced osteogenesis. Notch target gene Hey1 inhibits mineralization and Runx2 transcriptional activity. J Biol Chem 2004;**279**(36):37704-15 doi: 10.1074/jbc.M403813200[published Online First: Epub Date]|.

20. Chesi A, Wagley Y, Johnson ME, et al. Genome-scale Capture C promoter interactions implicate effector genes at GWAS loci for bone mineral density. Nat Commun 2019;**10**(1):1260 doi: 10.1038/s41467-019-09302-x[published Online First: Epub Date]|.

21. Wagley Y, Law PY, Wei LN, Loh HH. Epigenetic Activation of mu-Opioid Receptor Gene via Increased Expression and Function of Mitogen- and Stress-Activated Protein Kinase 1. Mol Pharmacol 2017;**91**(4):357-72 doi: 10.1124/mol.116.106567[published Online First: Epub Date]|.

22. Dobin A, Davis CA, Schlesinger F, et al. STAR: ultrafast universal RNA-seq aligner. Bioinformatics 2013;**29**(1):15-21 doi: 10.1093/bioinformatics/bts635[published Online First: Epub Date]|.

23. Wagley Y, Hwang CK, Lin HY, et al. Inhibition of c-Jun NH2-terminal kinase stimulates mu opioid receptor expression via p38 MAPK-mediated nuclear NF-kappaB activation in neuronal and non-neuronal cells. Biochim Biophys Acta 2013;**1833**(6):1476-88 doi: 10.1016/j.bbamcr.2013.02.017[published Online First: Epub Date]|.

24. Gifford GB, Demitrack ES, Keeley TM, et al. Notch1 and Notch2 receptors regulate mouse and human gastric antral epithelial cell homoeostasis. Gut 2017;**66**(6):1001-11 doi: 10.1136/gutjnl-2015-310811[published Online First: Epub Date]|.

25. Luo W, Friedman MS, Hankenson KD, Woolf PJ. Time series gene expression profiling and temporal regulatory pathway analysis of BMP6 induced osteoblast differentiation and

mineralization. BMC Syst Biol 2011;**5**:82 doi: 10.1186/1752-0509-5-82[published Online First: Epub Date]|.

26. Friedman MS, Long MW, Hankenson KD. Osteogenic differentiation of human mesenchymal stem cells is regulated by bone morphogenetic protein-6. J Cell Biochem 2006;**98**(3):538-54 doi: 10.1002/jcb.20719[published Online First: Epub Date]|.
27. Zhu F, Friedman MS, Luo W, Woolf P, Hankenson KD. The transcription factor osterix (SP7) regulates BMP6-induced human osteoblast differentiation. J Cell Physiol 2012;**227**(6):2677-85 doi: 10.1002/jcp.23010[published Online First: Epub Date]|.
28. Tanaka M, Nanba D, Mori S, et al. ADAM binding protein Eve-1 is required for ectodomain shedding of epidermal growth factor receptor ligands. J Biol Chem 2004;**279**(40):41950-9 doi: 10.1074/jbc.M400086200[published Online First: Epub Date]|.
29. Dishowitz MI, Terkhorn SP, Bostic SA, Hankenson KD. Notch signaling components are upregulated during both endochondral and intramembranous bone regeneration. J Orthop Res 2012;**30**(2):296-303 doi: 10.1002/jor.21518[published Online First: Epub Date]|.
30. Komori T. Regulation of Proliferation, Differentiation and Functions of Osteoblasts by Runx2. Int J Mol Sci 2019;**20**(7) doi: 10.3390/ijms20071694[published Online First: Epub Date]|.
31. Wang C, Inzana JA, Mirando AJ, et al. NOTCH signaling in skeletal progenitors is critical for fracture repair. J Clin Invest 2016;**126**(4):1471-81 doi: 10.1172/JCI80672[published Online First: Epub Date]|.

32. Tsuji K, Bandyopadhyay A, Harfe BD, et al. BMP2 activity, although dispensable for bone formation, is required for the initiation of fracture healing. Nat Genet 2006;**38**(12):1424-9 doi: 10.1038/ng1916[published Online First: Epub Date]|.

33. Canalis E. Notch signaling in osteoblasts. Sci Signal 2008;**1**(17):pe17 doi: 10.1126/stke.117pe17[published Online First: Epub Date]|.

34. Lin GL, Hankenson KD. Integration of BMP, Wnt, and notch signaling pathways in osteoblast differentiation. J Cell Biochem 2011;**112**(12):3491-501 doi: 10.1002/jcb.23287[published Online First: Epub Date]|.

35. Xu N, Liu H, Qu F, et al. Hypoxia inhibits the differentiation of mesenchymal stem cells into osteoblasts by activation of Notch signaling. Exp Mol Pathol 2013;**94**(1):33-9 doi: 10.1016/j.yexmp.2012.08.003[published Online First: Epub Date]|.

36. Hanai J, Chen LF, Kanno T, et al. Interaction and functional cooperation of PEBP2/CBF with Smads. Synergistic induction of the immunoglobulin germline Calpha promoter. J Biol Chem 1999;**274**(44):31577-82 doi: 10.1074/jbc.274.44.31577[published Online First: Epub Date]|.

37. Hakelien AM, Bryne JC, Harstad KG, et al. The regulatory landscape of osteogenic differentiation. Stem Cells 2014;**32**(10):2780-93 doi: 10.1002/stem.1759[published Online First: Epub Date]|.

38. Youngstrom DW, Dishowitz MI, Bales CB, et al. Jagged1 expression by osteoblast-lineage cells regulates trabecular bone mass and periosteal expansion in mice. Bone 2016;**91**:64-74 doi: 10.1016/j.bone.2016.07.006[published Online First: Epub Date]|.

LEGENDS FOR FIGURES

Figure 1:

Runx2 knockdown impairs human osteoblast differentiation in response to both Jagged1 and BMP2. (A-B) Runx2 siRNA transfected hMSC were stimulated with or without Jagged1 **(A)** or BMP2 **(B)** for 3 days and alkaline phosphatase expression was histochemically determined. Bottom histogram depict mean value of staining results using quantitative imaging from three independent donor lines. **(C-D)** Extracellular calcium deposition was histochemically determined by Alizarin red S staining of Runx2 siRNA transfected cells stimulated with or without Jagged1 **(C)** or BMP2 **(D)** for 10-12 days. Bottom histogram depict mean value of staining results using quantitative imaging from three independent donor lines. **(E)** Protein expression of Runx2, Osterix and RBPJ were determined in Runx2 siRNA transfected cells stimulated with or without BMP2 for 3 days. The levels of GAPDH was used as a loading control. Relative band densities for Runx2 **(F)** and Osterix **(G)** were determined using four different donor lines. **(H)** Protein levels of Runx2, Osterix, and RBPJ were determined in Runx2 siRNA transfected cells stimulated with or without Jagged1 for 3 days. The levels of GAPDH was used as loading control. Relative band densities for Runx2 **(F)** and Osterix **(G)** were determined using four independent experiments from two independent donor lines. Columns = mean. Error bars = Standard deviation. *p<0.05 comparing No treatment to respective

treatment with Jagged1 or BMP2 for each siRNA, #$p < 0.05$ comparing control siRNA to siRNA for gene of interest (two-way homoscedastic Student's *t*-tests).

Figure 2:

Notch signaling components are upregulated by both BMP and Jagged1 stimulation of human mesenchymal stem cells. (A) Total RNA samples prepared from three unique hMSC donor lines stimulated with BMP2 or Jagged1 for 3 days in osteogenic media were subjected to RNA sequencing on the Illumina NovaSeq platform. Total number of differentially expressed genes at a false discovery rate of <10% for each treatment group relative to its control group is shown (upregulated (upward facing green arrow), downregulated (downward facing arrow), and total (central oval)). **(B)** Venn diagrams of total number of commonly overlapping BMP2 and Jagged1 upregulated genes (45) shown in blue and downregulated genes (69) shown in red were determined by intersecting the data for upregulated genes and downregulated genes (FC>1.5) under each treatment condition. **(C)** Ingenuity Pathway Analysis of the top 10 genes out of the 45 commonly upregulated genes are depicted, and **(D)** Categorization of the top 10 commonly upregulated gene by biological processes.

Figure 3:

Gamma-secretase inhibitor impairs BMP-mediated human osteoblast differentiation. (A) Cells were stimulated with BMP2 or BMP6 (300 ng/ml) and immediately treated with DAPT or DAPT treated after 8h, 24h, 48h and 72h of the initial BMP stimulation. At the end of 96h after initial BMP exposure, alkaline phosphatase expression was histochemically determined. **(B)** Extracellular calcium deposition was histochemically determined after 10 days by Alizarin red S staining of cells stimulated as above. **(C-F)** Quantitative gene expression of *ID1, ALPL, HEY2* and *HES4* in hMSCs stimulated for 72h with BMP2 with or without DAPT. **(G)** Protein expression of P-SMAD1/5/9, Runx2, Osterix, Notch1 (val 1744), Notch2 (NTM), Notch3 (FL), and Notch3 (NTM) were determined in cells stimulated with BMP2 in presence or absence of DAPT for 72h. The levels of GAPDH was used as a loading control. Relative band densities for P-SMAD1/5/9 **(H)**, Runx2 **(I)**, Osterix **(J)** and Notch3 (NTM) were calculated using three different donor lines. Gray columns = No DAPT; Black columns = DAPT treatment. Columns = mean. Error bars = Standard deviation. *$p<0.05$ comparing No treatment to BMP2 treatment, #$p < 0.05$ comparing control siRNA to siRNA for gene of interest, n.s = not significant (two-way homoscedastic Student's *t*-tests).

Figure 4:

Notch activation and Osterix protein expression co-occur with alkaline phosphatase expression in BMP2 stimulated human mesenchymal stem cells. (A) Experimental outline to

determine the effect of BMP washout in alkaline phosphatase expression. **(B)** Cells were stimulated with BMP2 and at the indicated times received two washes with osteogenic media from indicated wells. After a total of 96h after initial BMP stimulation, alkaline phosphatase expression was determined by histochemical staining. Right histogram depicts relative alkaline phosphatase expression determined by quantitative image analysis of the stained wells depicted in **(B)**. For the well stimulated with BMP2 without any washout for 96h, the levels of alkaline phosphatase expression level were arbitrarily set at 100%. **(C-D)** Quantitative gene expression of **(C)** *ID1* and **(D)** *ALPL* was determined in cells stimulated with BMP for up to 96h as indicated. **(E)** Protein expression of P-SMAD1/5/9, Osterix, Notch1 (VAL 1744), Notch2 (NTM) and Notch3 (NTM) were determined in BMP stimulated cells for indicated times. GAPDH was used as internal control. $*p<0.05$ comparing No treatment to BMP2 treatment, $\#p < 0.05$ comparing No washout to washout at indicated times, n.s = not significant (two-way homoscedastic Student's *t*-tests).

Figure 5:

Canonical Notch signaling via RBPJ is required for BMP mediated human osteoblast differentiation. (A) RBPJ siRNA transfected hMSC were stimulated with or without BMP2 for 3 days and alkaline phosphatase expression was histochemically determined. **(B)** Extracellular calcium deposition was histochemically determined by alizarin red S staining of RBPJ siRNA

transfected cells stimulated with or without BMP2 for 10 days. **(C)** Quantitative image analysis from three independent hMSC donor lines to determine relative alkaline phosphatase expression in RBPJ siRNA transfected cells. **(D)** Quantitative image analysis from four independent hMSC donor lines were combined to determine relative mineralization levels. **(E)** Protein levels of RBPJ, P-SMAD1/5/9, Runx2 and Osterix were determined in RBPJ siRNA transfected cells stimulated with or without BMP2 for 72 hours. The levels of GAPDH were used as internal control. **(F-H)** Densitometric analysis of immunoblot experiments as in **(E)** from three independent donor lines were performed to enumerate relative band densities for RBPJ **(F)**, Runx2 **(G)**, and Osterix **(H)**. **(I-L)** Quantitative gene expression analysis to determine relative expression levels of *ID1* **(I)**, *ALPL* **(J)**, *JAG1* **(K)**, and *HEY2* **(L)** in four independent hMSC donor lines after RBPJ silencing. Gray columns = No BMP; Black columns = BMP treatment. Columns = mean. Error bars = Standard deviation. *$p<0.05$ comparing No treatment to BMP2 treatment, #$p < 0.05$ comparing control siRNA to RBPJ siRNA (two-way homoscedastic Student's *t*-tests).

Figure 6:

RBPJ is bound at the human *ALPL* and *SP7* promoter regions. (A) Upper panel: Schematic depiction of chromatin immunoprecipitation (ChIP) primer locations (arrowheads) in the human *HES1* promoter region. Location +1 and a turning arrow above it represents the transcription start

site. Lower histogram: hMSC were stimulated with or without BMP2 for 3 days in serum-free osteogenic media and chromatin immunoprecipitation (ChIP) was performed with either normal rabbit IgG or anti-RBPJ antibody. Relative enrichment of DNA compared to input samples were calculated for each immunoprecipitation reaction and presented. **(B-E)** Schematic representation of ChIP primer locations and relative enrichment of DNA compared to input samples around **(B)** ***HEY1***, **(C)** ***ALPL***, **(D)** ***SP7*** and **(E)** ***RUNX2*** gene. ChIP experiments were performed in 3 independent hMSC donor lines. Gray columns = No BMP; Black columns = BMP treatment. Columns = mean. Error bars = Standard deviation. *$p<0.05$ comparing normal rabbit IgG to RBPJ antibody (two-way homoscedastic Student's *t*-tests).

Figure 7:

Pharmacological Notch inhibition using dibenzazepine (DBZ) reduces bone volume during BMP2 mediated calvarial defect healing of mice. (A) Representative microCT images taken at day 42 of calvarial defects of a vehicle and DBZ treated mouse. All 18 animals received 0.25µg BMP2 on the day of calvarial defect surgery and received intraperitoneal injections of either vehicle (n=9) or DBZ (n=9) on days 5-9 after the surgery. **(B)** Bone volume (BV) was measured across animals that received vehicle or DBZ injections as described above. *$p<0.05$ comparing vehicle control to DBZ treated group (two-way homoscedastic Student's *t*-tests)

FIG. 1

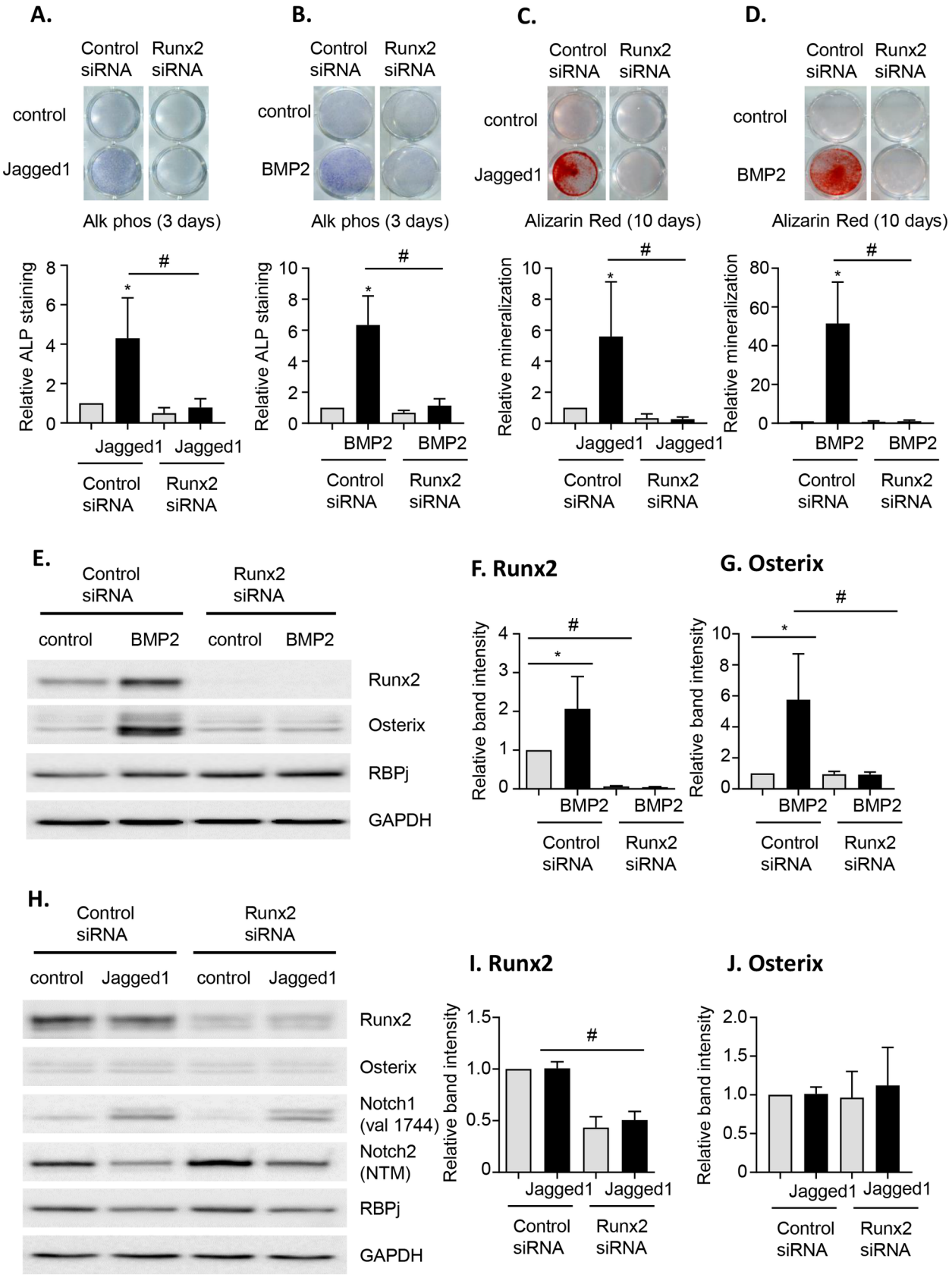

STEM_3245_FIGURE 1.tif

FIG. 2

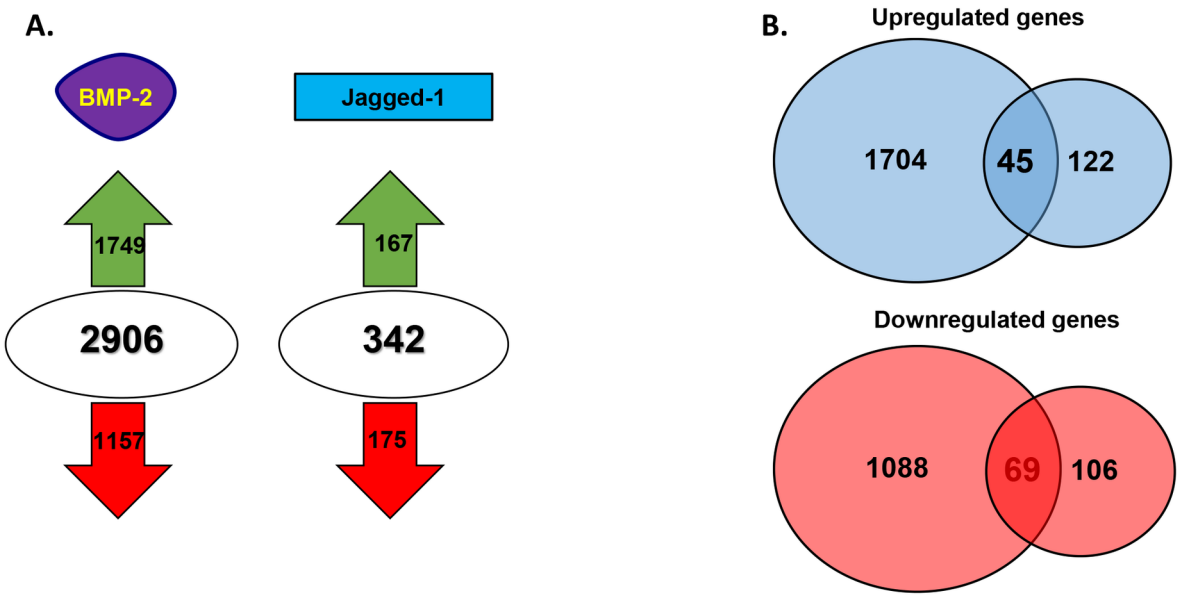

C.

Name	p. Value	Overlap
Notch signaling	4.57E-05	8.1% (3/37)
Regulation of the Epithelial-Mesenchymal Transition Pathway	4.10E-04	2.1% (4/187)
Osteoarthritis Pathway	5.90E-04	1.9% (4/206)
RhoA Signaling	2.21E-02	1.6% (2/122)
Epithelial Adherens Junction Signaling	2.97E-02	1.4% (2/143)

D.

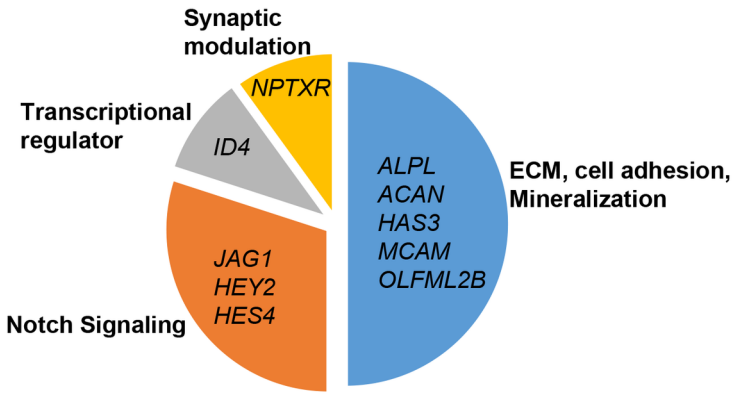

STEM_3245_FIGURE 2.tif

FIG. 3

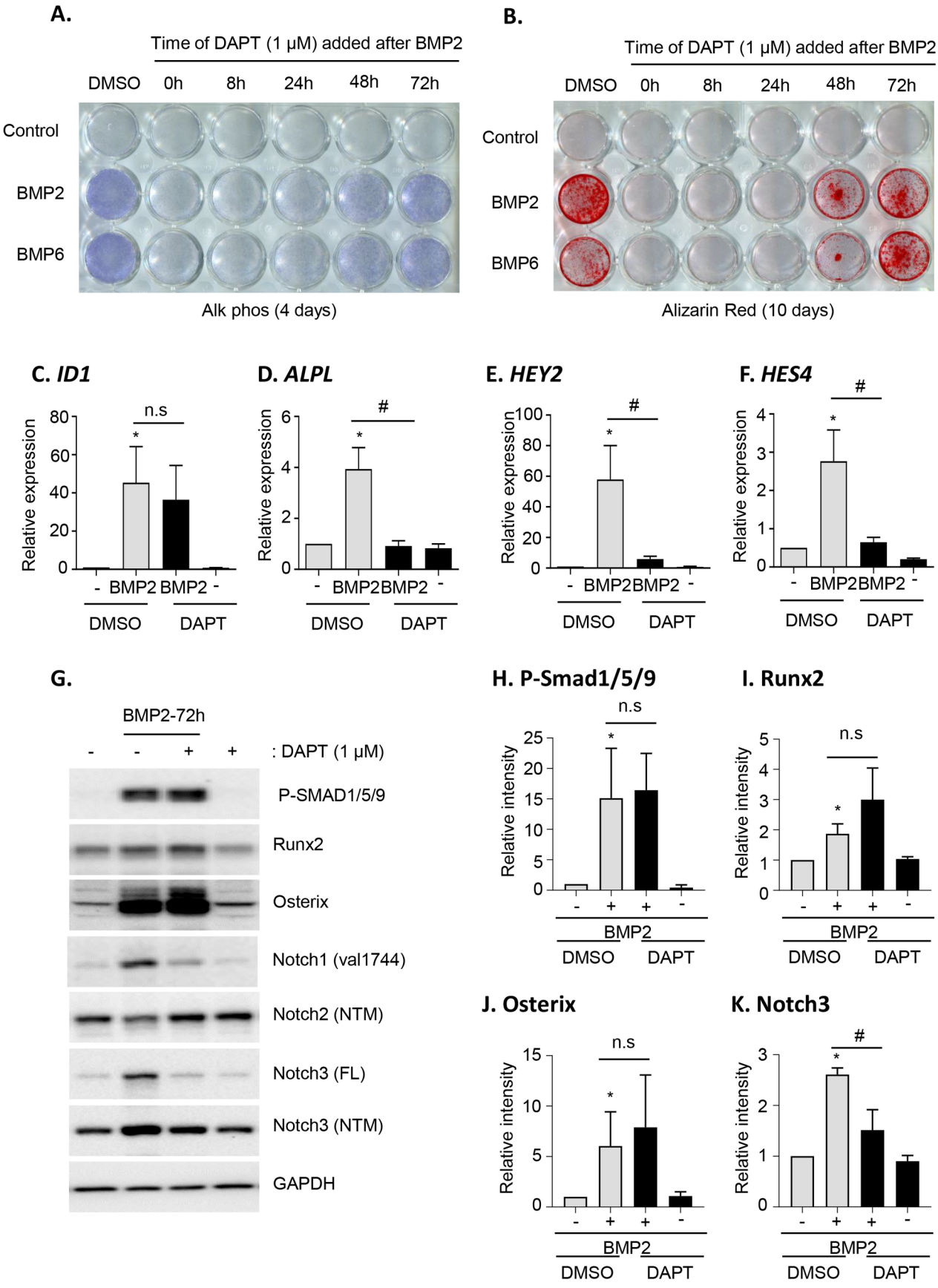

STEM_3245_FIGURE 3.tif

FIG. 4

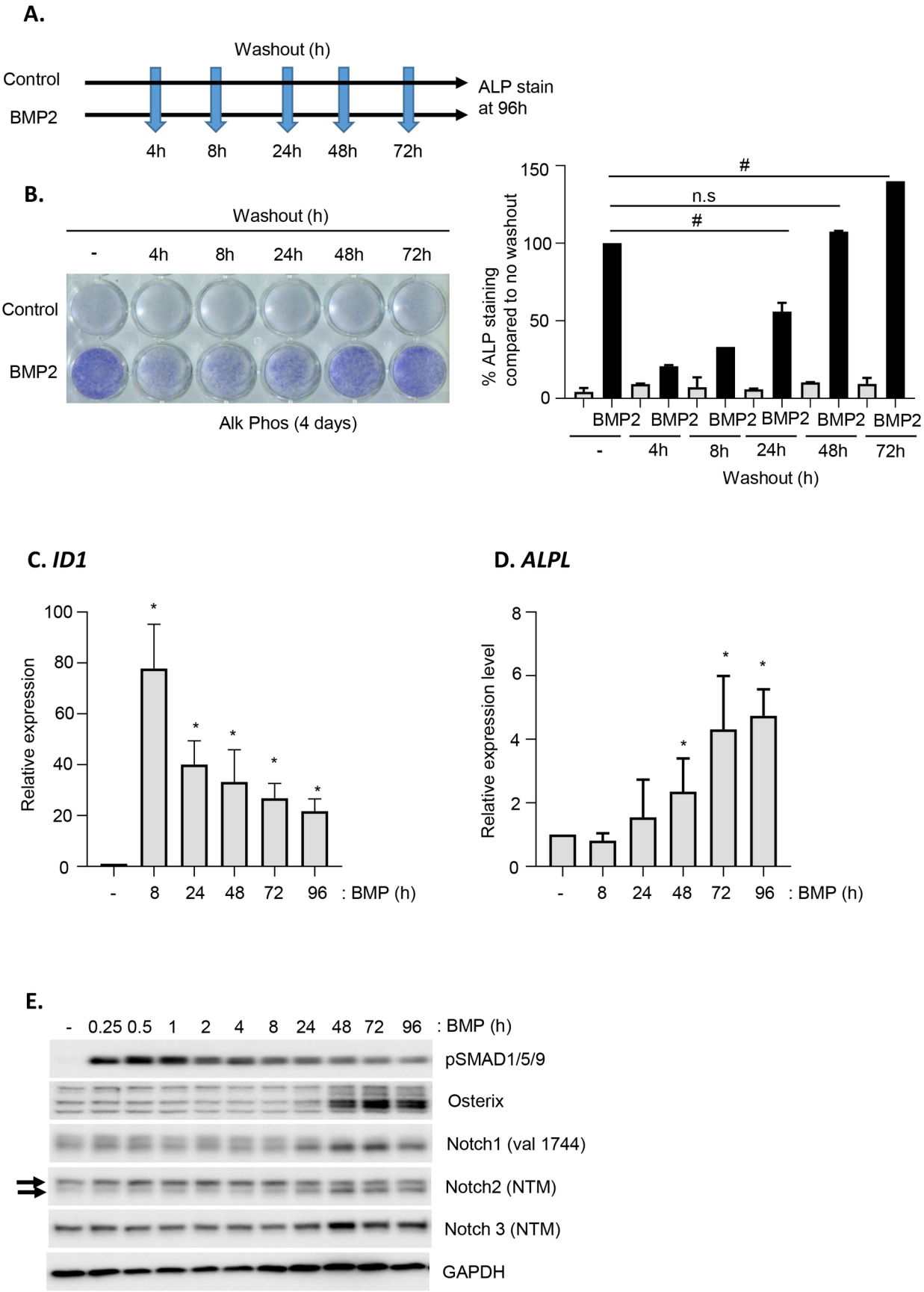

STEM_3245_FIGURE 4.tif

FIG. 5

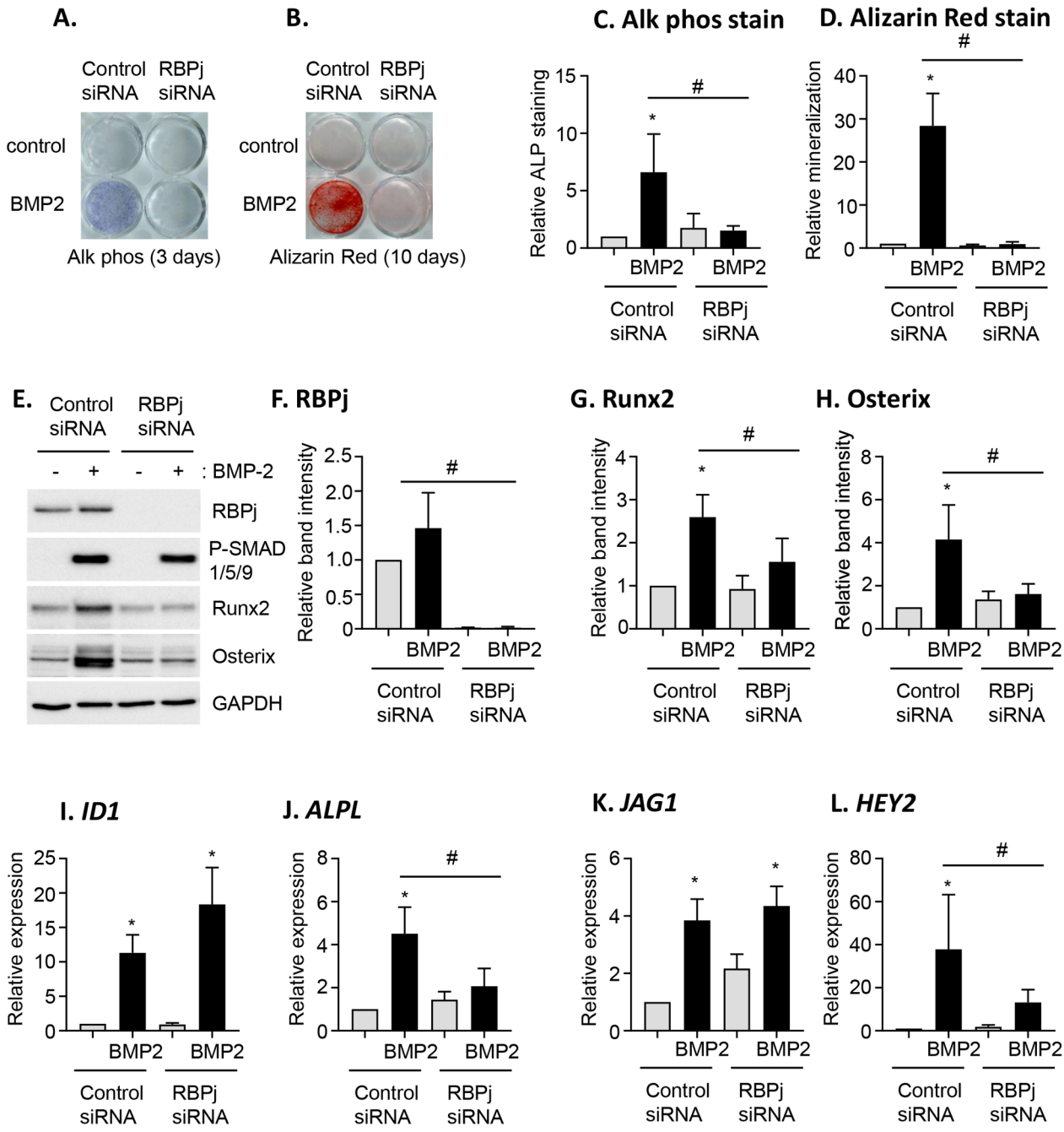

STEM_3245_FIGURE 5.tif

FIG. 6

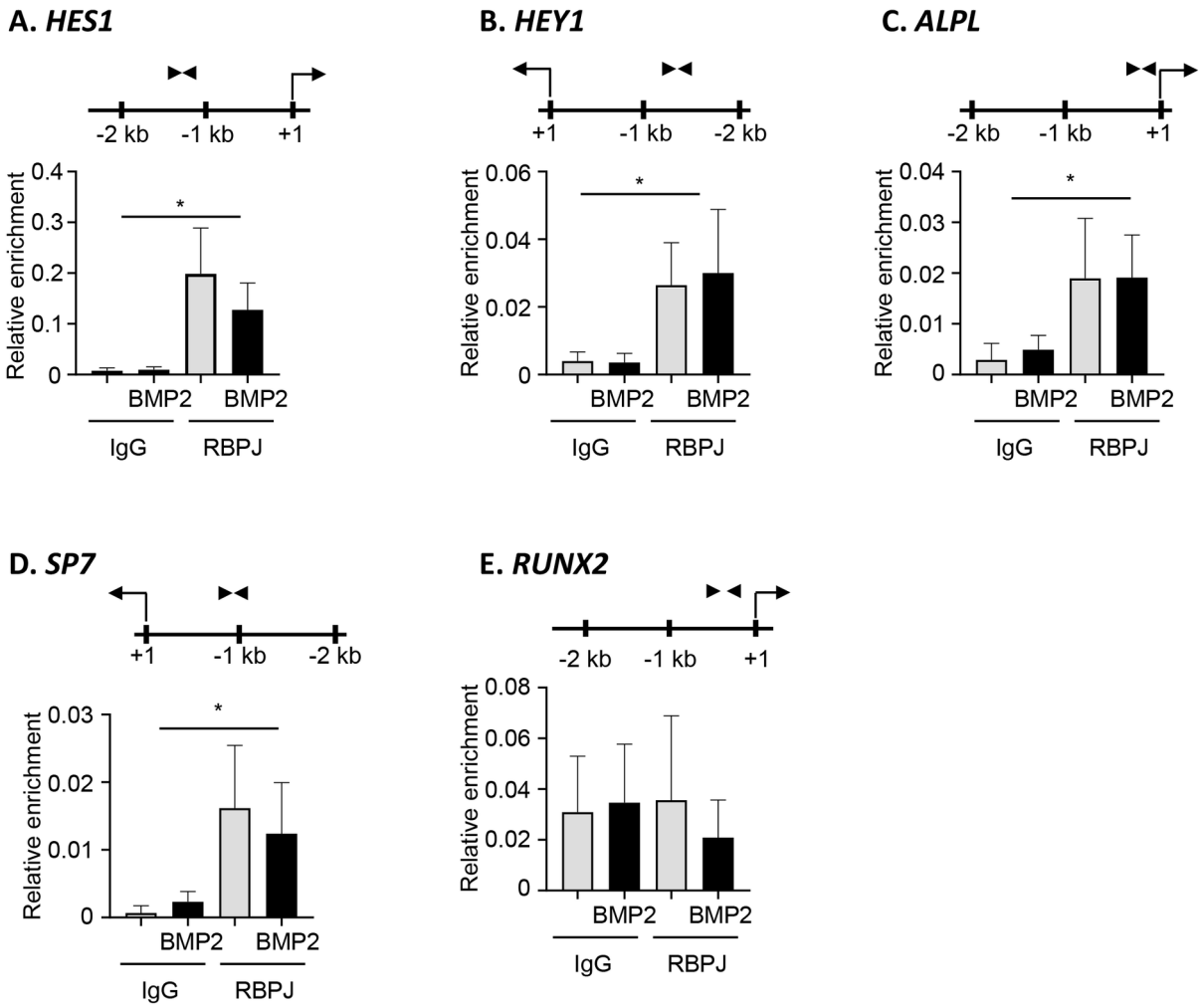

STEM_3245_FIGURE 6.tif

FIG. 7

A.

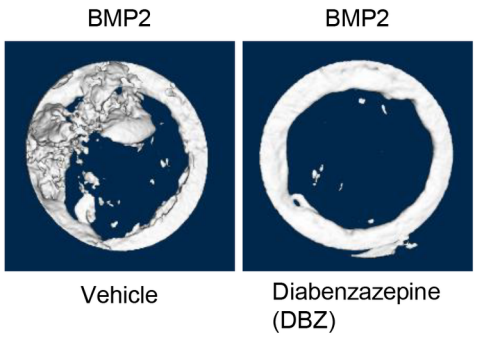

B. *Bone Volume*

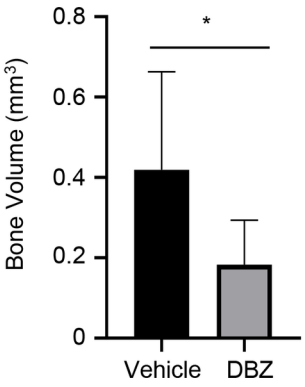

STEM_3245_FIGURE 7.tif

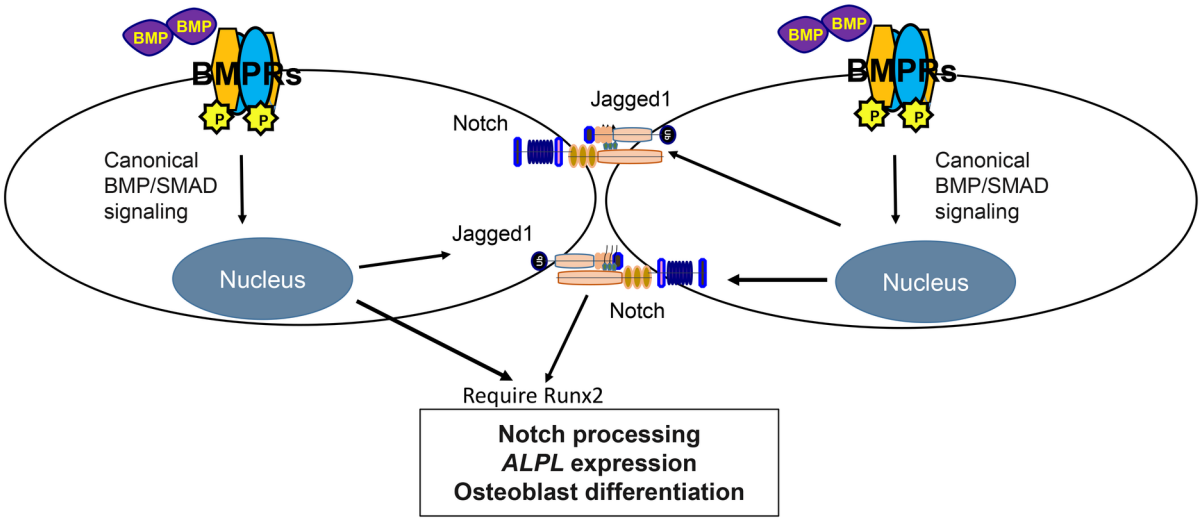

STEM_3245_Graphical_abstract.tif

STEM CELLS®

POTENTIAL CONFLICT OF INTEREST AND FINANCIAL DISCLOSURE FORM – AUTHOR

It is the policy of STEM CELLS® Journal to ensure balance, independence, objectivity, and scientific rigor in all of its educational activities through the disclosure of financial interests and other relationships.

POLICY: In accordance with Journal policy, all persons who affect the content of an article regarding the products or services of a commercial interest must disclose any financial relationships with that commercial interest occurring within the last 12 months. STEM CELLS® abides by a policy of anonymous peer review: any potential conflicts of interest are reviewed by the Editorial Board with the ad hoc assistance of external reviewers and are resolved prior to publication.

DEFINING A CONFLICT OF INTEREST: A conflict of interest exists when an individual has both **a financial relationship** with a commercial interest and **the opportunity to affect the content of an article** about the product or services of that commercial interest. STEM CELLS® has faith in the integrity of the individuals who present educational activities. However, to avoid the appearance of any conflict of interest, this form has been adopted to identify and resolve any potential conflicts of interest.

CRITERIA FOR FINANCIAL DISCLOSURE: A *commercial interest* is defined as any entity producing, marketing, re-selling, or distributing health care goods or services consumed by, or used on, patients. Relationships with governmental agencies (e.g., the National Institutes of Health) do not have to be disclosed. Principal investigators must report research funding relationships under "Research" even if those funds were disbursed to an institution. In addition to your own disclosure, you must disclose financial relationships your spouse or life partner has with applicable commercial interests. A spouse or life partner's disclosure information should be included with your disclosure information in the table below (and marked accordingly).

Manuscript Title: Canonical Notch Signaling is Required for Bone Morphogenetic Protein-mediated Human Osteoblast Differ

Name of Discloser: Yadav Wagley

I am a: ☐ Co-Author ☑ Corresponding Author

Do you have any financial relationships to report?
☐ **Yes** ☑ **No**

If yes, please provide relevant information in table below.

Types of financial relationships and the companies with whom we (I and/or my spouse/life partner) have relationships are as follows:

Check boxes	Type of financial relationship WITHIN THE PAST 12 MONTHS ONLY	Indicate applicable commercial interest(s) WITHIN THE PAST 12 MONTHS ONLY	Compensated ✓	Uncompensated ✓
☐	Employment/leadership position		☐	☐
☐	Intellectual property rights/Inventor or patent holder		☐	☐
☐	Consultant/Advisory role		☐	☐
☐	Honoraria received directly from commercial interest or their agents (e.g., speakers' bureaus)		☐	☐
☐	Research funding/Contracted research (including funds paid to your institution)		☐	☐
☐	Ownership interest (stocks, stock options, or other ownership interest excluding diversified mutual funds)		☐	☐
☐	Expert testimony		☐	☐
☐	Other (including any reimbursed or sponsored travel)		☐	☐

If you reported relationships in the chart above, will you nonetheless be able to provide an unbiased article? ☐ **Yes** ☐ **No**

By signing below, I represent that the foregoing information is complete and truthful. I will notify the editorial office if there are any changes in my financial relationships prior to the publication of this article.

Yadav Wagley
Signature of Reporting Individual

01/07/2020
Date of Submission

Rev. 3-11-14

STEM CELLS®

POTENTIAL CONFLICT OF INTEREST AND FINANCIAL DISCLOSURE FORM – AUTHOR

It is the policy of STEM CELLS® Journal to ensure balance, independence, objectivity, and scientific rigor in all of its educational activities through the disclosure of financial interests and other relationships.

POLICY: In accordance with Journal policy, all persons who affect the content of an article regarding the products or services of a commercial interest must disclose any financial relationships with that commercial interest occurring within the last 12 months. STEM CELLS® abides by a policy of anonymous peer review: any potential conflicts of interest are reviewed by the Editorial Board with the ad hoc assistance of external reviewers and are resolved prior to publication.

DEFINING A CONFLICT OF INTEREST: A conflict of interest exists when an individual has both **a financial relationship** with a commercial interest and **the opportunity to affect the content of an article** about the product or services of that commercial interest. STEM CELLS® has faith in the integrity of the individuals who present educational activities. However, to avoid the appearance of any conflict of interest, this form has been adopted to identify and resolve any potential conflicts of interest.

CRITERIA FOR FINANCIAL DISCLOSURE: A *commercial interest* is defined as any entity producing, marketing, re-selling, or distributing health care goods or services consumed by, or used on, patients. Relationships with governmental agencies (e.g., the National Institutes of Health) do not have to be disclosed. Principal investigators must report research funding relationships under "Research" even if those funds were disbursed to an institution. In addition to your own disclosure, you must disclose financial relationships your spouse or life partner has with applicable commercial interests. A spouse or life partner's disclosure information should be included with your disclosure information in the table below (and marked accordingly).

Manuscript Title:

Name of Discloser: Kurt D. Hankenson

I am a: ☐ Co-Author ☑ Corresponding Author

Do you have any financial relationships to report?
☐ **Yes** ☑ **No**

If yes, please provide relevant information in table below.

Types of financial relationships and the companies with whom we (I and/or my spouse/life partner) have relationships are as follows:

Check boxes	Type of financial relationship WITHIN THE PAST 12 MONTHS ONLY	Indicate applicable commercial interest(s) WITHIN THE PAST 12 MONTHS ONLY	Compensated ✓	Uncompensated ✓
☐	Employment/leadership position		☐	☐
☐	Intellectual property rights/Inventor or patent holder		☐	☐
☐	Consultant/Advisory role		☐	☐
☐	Honoraria received directly from commercial interest or their agents (e.g., speakers' bureaus)		☐	☐
☐	Research funding/Contracted research (including funds paid to your institution)		☐	☐
☐	Ownership interest (stocks, stock options, or other ownership interest excluding diversified mutual funds)		☐	☐
☐	Expert testimony		☐	☐
☐	Other (including any reimbursed or sponsored travel)		☐	☐

If you reported relationships in the chart above, will you nonetheless be able to provide an unbiased article? ☑ **Yes** ☐ **No**

By signing below, I represent that the foregoing information is complete and truthful. I will notify the editorial office if there are any changes in my financial relationships prior to the publication of this article.

Digitally signed by Kurt D Hankenson
Date: 2020.01.07 06:56:34 -05'00'

Signature of Reporting Individual

Date of Submission

Rev. 3-11-14